

Analysis and Optimization of a Novel Consequent Pole Flux Reversal Machine with Asymmetric-Stator-Poles

Libing Jing* and Kun Yang

Abstract—Flux reversal machines (FRMs) have a broad application prospect due to their simple structure, high efficiency, and high reliability. However, due to the large magnetic flux leakage between poles, the further improvement of torque density of the FRMs is limited. To reduce magnetic flux leakage and improve torque, a novel consequent pole FRM with asymmetric stator poles is proposed in this paper. The ‘NS-NS’ arrangement order of the permanent magnets (PMs) of the conventional FRM is changed to the ‘NSN-S’ PMs arrangement order with asymmetric stator poles, and the consequent pole topology is used simultaneously. All the N-poles of PMs are replaced by iron poles. Finally, the topology of the ‘Fe/S/Fe-S’ arrangement order is obtained. A simplified magnetic circuit model is established to explain the principle of reducing magnetic flux leakage. To improve the torque density, the key design parameters are optimized by genetic algorithm, and the optimal parameters of the machine are finally determined. Finally, the finite element model is established. Compared with the conventional FRM, the torque of the proposed machine is increased by 67.18%, and the consumption of PM is reduced by 51.6%. Therefore, the proposed machine has good electromagnetic characteristics and economic benefits.

1. INTRODUCTION

The permanent magnet (PM) machines can be divided into rotor PM machines and stator PM machines according to different positions of PMs [1]. The conventional rotor PM machines have the advantages of high efficiency in practical application. However, due to the difficulty in cooling of the PM on a rotor during operation, it has the disadvantages of high risk of demagnetization and poor reliability, which limits the further improvement of its machine performance. To overcome some inherent problems of the rotor PM machines and further improve the machine performance, the stator PM machines with PMs on the stator have attracted wide attention from most scholars. The PM and winding of the stator PM machines are on the static stator, and the rotor is a very simple salient pole structure. PMs do not require complex processes to be fixed, and the heat dissipation of the machine is more convenient, with its reliability improved significantly.

As one of the typical representatives of stator PM machines, flux reversal machines (FRMs) have been successfully applied to electric vehicles, new energy power generation, and many other occasions [2, 3]. FRMs have attracted more and more attention in recent years due to their simple structure, high efficiency, and high reliability. In [4], the effects of different magnetization modes and coil pitches on the back EMF of the FRMs are studied. In [5], based on the magnetomotive force — permeance model, the back EMF of FRMs is analyzed by using the magnetic field modulation theory, to obtain the reasonable magnetization mode, winding arrangement, and number of rotor poles. In [6], the optimal number of PMs on each stator tooth of the FRMs is studied. It is found that compared with the two PMs on each stator tooth, the optimal number of PMs can significantly improve the torque,

Received 8 September 2022, Accepted 2 November 2022, Scheduled 11 November 2022

* Corresponding author: Libing Jing (jinglibing163@163.com).

The authors are with the College of Electrical Engineering & New Energy, China Three Gorges University, Yichang 443002, China.

and the optimal PM arrangement is further studied. In [7], an FRM with evenly distribution of PMs is proposed, the electromagnetic torque significantly increased, and the torque ripple reduced. In [8], an FRM with Halbach PMs at the opening of the stator slot is proposed. The machine reduces the length of the equivalent air gap to obtain a larger flux density, thus obtaining a larger electromagnetic torque at the same consumption of PM. In [9], a novel consequent pole FRM is proposed, which is characterized by that the number of iron poles under one stator tooth is larger than that of PM poles. The machine effectively improves the electromagnetic torque, but brings too large torque ripple, so some methods are used in the article to suppress torque ripple. In [10], an FRM with asymmetric stator is proposed, which improves the electromagnetic torque and reduces the torque ripple, and the power factor is also improved. In [11], FRMs with ring winding and concentrated winding are compared and analyzed, and the results show that the FRM with ring winding has good performance, including the torque, power factor, efficiency, and torque ripple. In [12], an FRM with spoke array PMs is proposed, which has higher torque, higher efficiency, and higher power factor than the conventional FRM. Then, the influence of the number and shape of PMs on the performance of the machine is studied. In [13], a doubly fed FRM is proposed. The machine has two independent windings in the rotor slot and stator slot, which effectively improves the torque performance and fault tolerance. In the subsequent study [14], the doubly fed FRM with Halbach array PM in the rotor slot is further proposed.

The conventional FRM has a lot of magnetic flux leakage every moment, which is a very serious constraint on the torque density of the machines. In previous studies, the structure of stator and rotor teeth was changed to reduce the magnetic flux leakage, such as concave surface of stator tooth, or rotor tooth was added with a section of air gap as the flux fence, but no satisfactory results were obtained. In this paper, a consequent pole FRM with asymmetric stator poles is proposed, which effectively reduces magnetic flux leakage and improves torque, while reducing the consumption of PM.

The structure of this paper is as follows. In Section 2, the topology and working principle of the machine are introduced. In Section 3, a simplified magnetic circuit model is established to explain the principle of reducing magnetic flux leakage. In Section 4, the sensitivity of design parameters is analyzed, and the parameters with high sensitivity are optimized by multi-objective optimization based on genetic algorithm to obtain optimal electromagnetic torque. In Section 5, the finite element model is established, and the electromagnetic performance is compared with that of the conventional FRM. In Section 6, this article is summarized, and the conclusions are drawn.

2. TOPOLOGY AND OPERATION PRINCIPLE

2.1. Topology

The conventional FRM with 12 slots and 17 poles has better torque quality than other number of poles and slots [15]. Based on the conventional 12 slots and 17 poles FRM shown in Figure 1(a), the topology of the novel 12 slots and 17 poles FRM is proposed as shown in Figure 1(b). The PM arrangement order of conventional FRM is alternating ‘NS-NS’. The novel topology is changed to the arrangement order of ‘NSN-S’ PMs with asymmetric stator teeth, and the consequent pole structure is simultaneously used to replace all N-pole PMs with iron materials. Finally, the topology of ‘Fe/S/Fe-S’ arrangement order is obtained.

2.2. OPERATION PRINCIPLE

The operation of FRMs is based on the magnetic field modulation theory. The static magnetomotive force is modulated by the rotor tooth to produce the rotary air gap magnetic density. With the rotation of the rotor, the change of the relative position between the stator and rotor brings about the change of the magnetic circuit. The magnetic field distribution of the machines at different rotor positions in an electric cycle is shown in Figure 2. The change of magnetic circuit makes the magnetic flux change in the coil, and then no-load back EMF is induced. In an electrical cycle, the flux linkage of each phase winding of the FRMs is reversed.

According to magnetic field modulation theory [16], the winding pole-pairs P , stator slot number

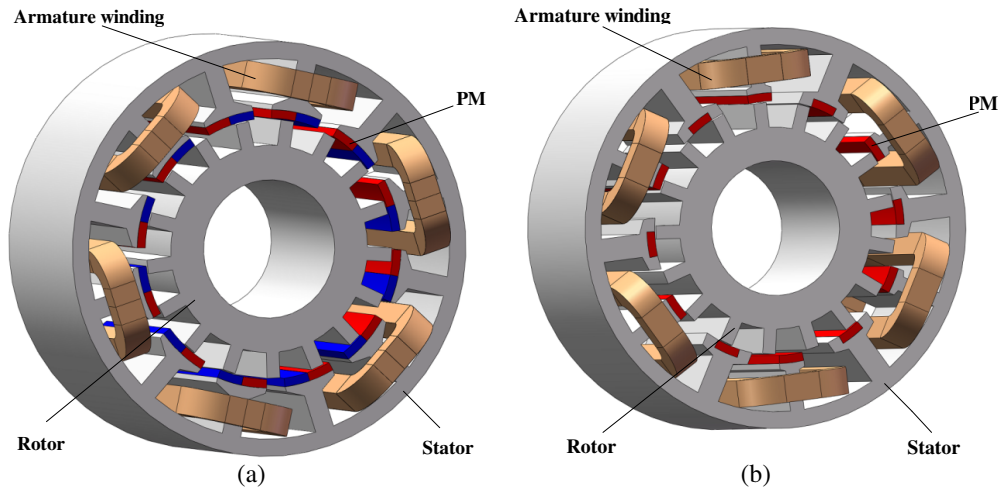


Figure 1. The topology of machines. (a) Conventional model; (b) Proposed model.

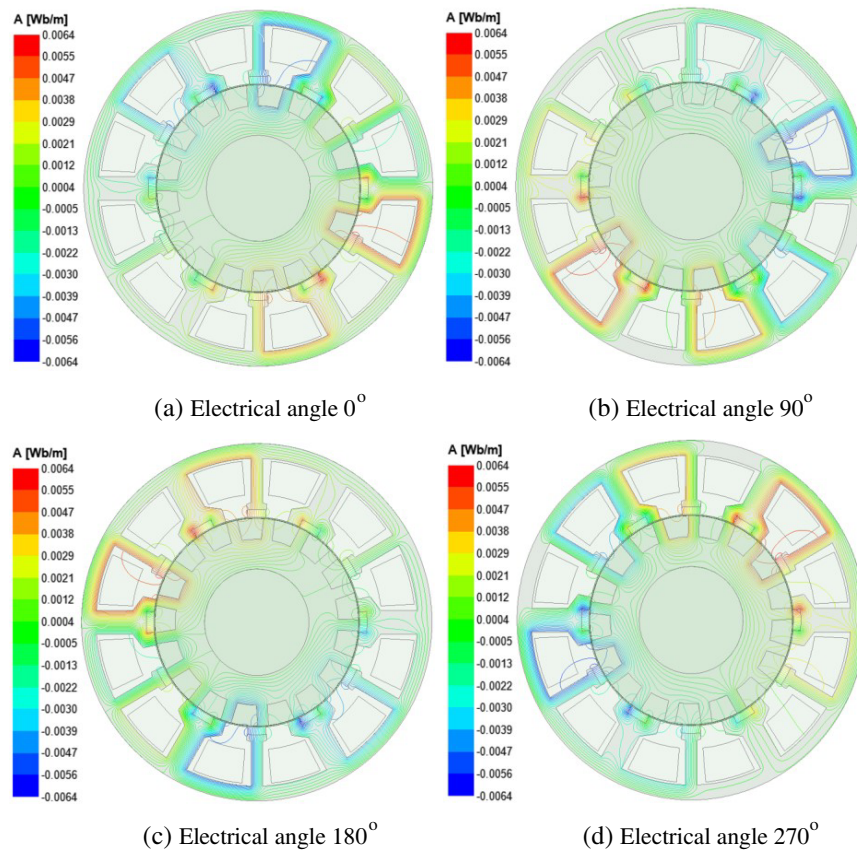


Figure 2. Flux lines distribution of FRMs at different rotor positions.

N_s , and rotor tooth number N_r of the FRM should satisfy:

$$P = \min \left\{ |nN_s \pm mN_r|; \frac{N_s}{\text{GCD}(N_s, P)} = 3j \right\} \quad (1)$$

where $n = 1, 2, 4, 5, \dots, k$, $k \neq 3i$ ($i = 1, 2, 3, \dots$), $m = 1, 2, 3, \dots$, $j = 1, 2, 3, \dots$, GCD denotes the greatest common divisor.

3. PRINCIPLE OF REDUCING MAGNETIC FLUX LEAKAGE

A simplified magnetic circuit model as shown in Figure 3 is established to clearly explain the principle of reducing magnetic flux leakage [9]. The magnetic flux leakage generated by the PM of the conventional FRM is shown in Figure 3(a). To reduce the magnetic flux leakage of the PM and increase the main flux, the magnetic flux leakage of the novel consequent pole FRMs with asymmetric stator teeth is shown in Figure 3(b).

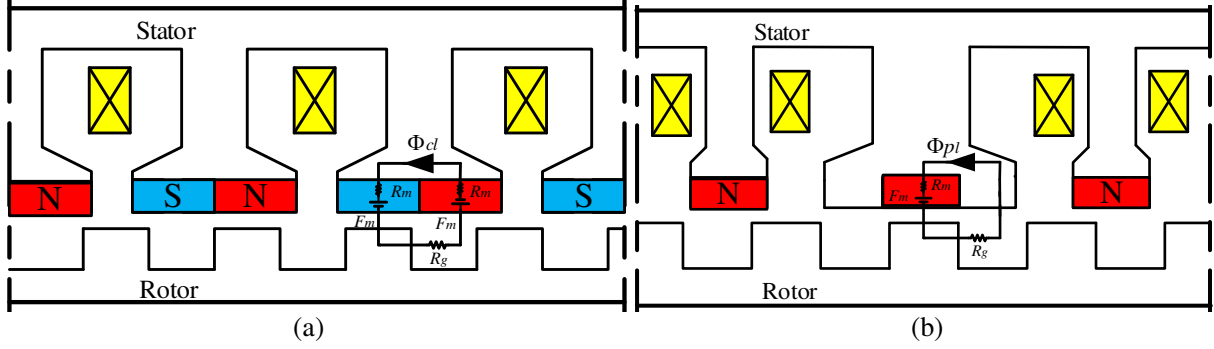


Figure 3. Simplified magnetic circuit model of FRMs. (a) Conventional model; (b) Proposed model.

The permeability of iron material is far greater than that of PM, and its magnetoresistance can be ignored in approximate estimation. Therefore, the magnetic flux leakage Φ_{cl} on each stator pole of the conventional FRM can be obtained:

$$\Phi_{cl} = \frac{2F_m}{2R_m + R_g} = \frac{F_m}{R_m + R_g/2} \quad (2)$$

where F_m is the magnetomotive force of a PMs, R_g the air gap magnetoresistance under a PM pole, and R_m the magnetoresistance of a PMs.

The total magnetic flux leakage Φ_{acl} of the conventional FRM can be obtained:

$$\Phi_{acl} = 12\Phi_{cl} = \frac{12F_m}{R_m + R_g/2} \quad (3)$$

The magnetic flux leakage of the proposed model is shown in Figure 3(b), and the magnetic flux leakage Φ_{pl} of the PMs on adjacent two stator poles of the proposed FRM can be obtained:

$$\Phi_{pl} = \frac{F_m}{2R_m + 2R_g} \quad (4)$$

The total magnetic flux leakage Φ_{pcl} of the proposed FRM can be obtained:

$$\Phi_{pcl} = 6\Phi_{pl} = \frac{3F_m}{R_m + R_g} \quad (5)$$

By comparison, the magnetic flux leakage Φ_{acl} of the conventional FRM is much larger than the magnetic flux leakage Φ_{pcl} of the proposed FRM, and the magnetic flux leakage of the proposed FRM is less than a quarter of that of the conventional machine. A decrease in magnetic flux leakage leads to an increase in the main flux resulting in greater flux linkage and torque.

4. PARAMETRIC OPTIMIZATION

To obtain better torque quality, the parameters of the machine are optimized by multi-objective optimization aiming at maximum electromagnetic torque and minimum torque ripple [17]. Before optimization, some parameters such as the total volume, current value, and material of the machine are determined and held constant, as listed in Table 1. Then, a full parametric model of the proposed

Table 1. Design parameters of the machine.

Parameter	value
Axial length	60 mm
Outer radius of machine	60 mm
Supplied current value	7 A
Number of coils per phase	60
Speed	3000 rpm
PMs material	NdFeB
Steel material	DW315-50

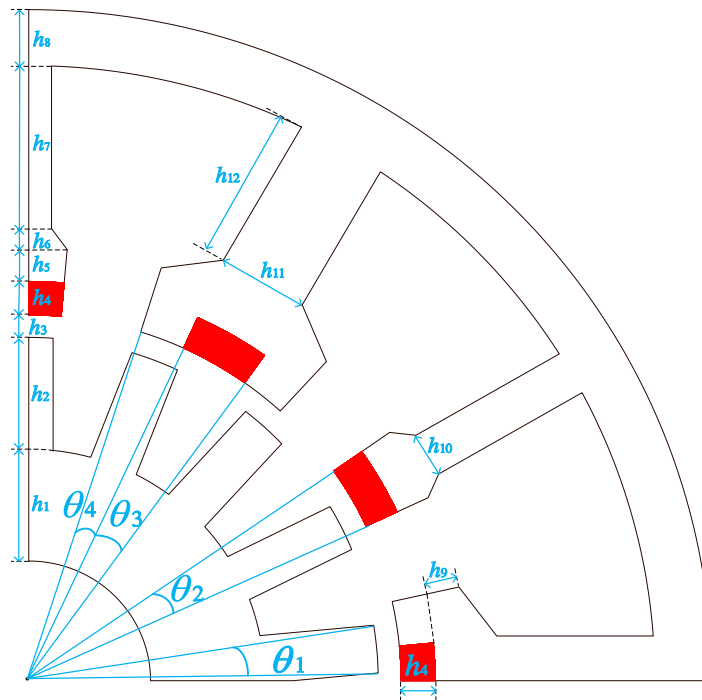


Figure 4. Parameterized model of the machine.

FRMs is established under the premise of determining the size constraint of the machines, and the design parameters are shown in Figure 4.

To save the optimization time effectively under the premise of ensuring the accuracy, the sensitivity analysis of all parameters is carried out, and the influence degree of different parameters on multiple optimization objectives is obtained. Then the parameters with high sensitivity are optimized by genetic algorithm. The flowchart of optimization is shown in Figure 5 [18].

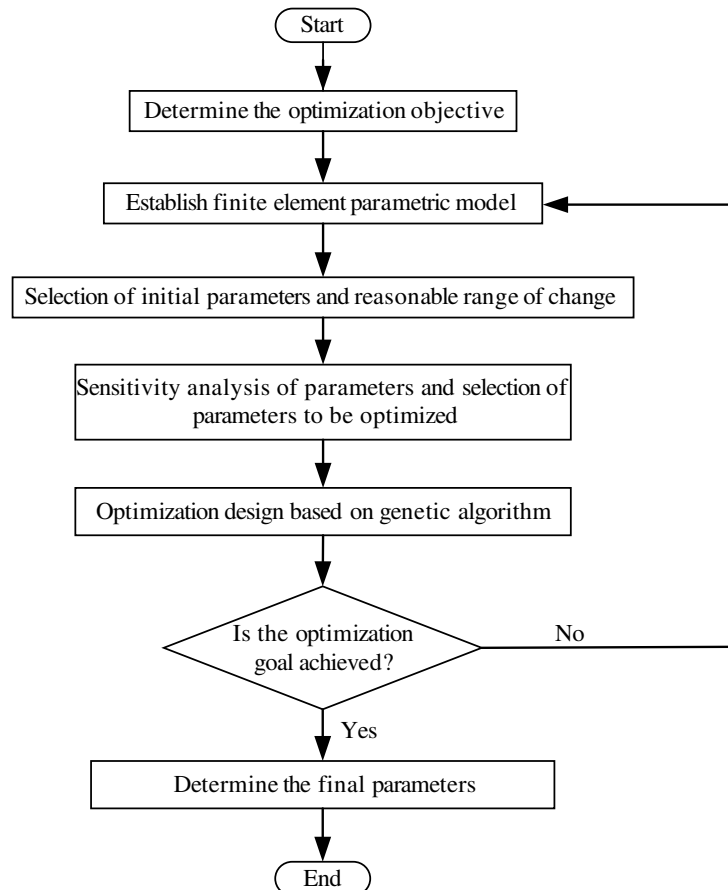
Genetic algorithm is a random search algorithm evolved from the natural selection mechanism in the biological world [19]. Considering the efficiency of optimization and the effectiveness of optimization results, the parameters of multiobjective genetic algorithm (MOGA) are as follows:

$$\begin{cases} \text{Population size} = 200 \\ \text{Generations} = 1000 \\ \text{Crossover probability} = 0.75 \\ \text{Mutation probability} = 0.05 \end{cases}$$

The Pareto front of MOGA is shown in Figure 6, and the optimal parameters of the machines are finally determined. The optimized parameters of the machine are listed in Table 2.

Table 2. Optimized parameters of the machine.

Parameter	Initial value	Value range	Terminal value
Thickness of rotor yoke h_1 /mm	10	7.5–12.5	10
Length of rotor tooth h_2 /mm	7	5–9	7
Length of air gap h_3 /mm	0.5	0.4–0.6	0.4
Thickness of PM h_4 /mm	2.5	2–3	2.5
Thickness of small stator tooth h_5 /mm	1.5	0.5–2.5	1.8
Thickness of small stator tooth edge h_6 /mm	1.5	0–3	0.5
Length of small stator tooth h_7 /mm	17	13–20	15.9
Thickness of stator yoke h_8 /mm	5	3–10	5
Thickness of large stator tooth edge h_9 /mm	1.5	0.5–2.5	1.8
Width of small stator tooth h_{10} /mm	4	2–6	4
Width of large stator tooth h_{11} /mm	8	4–12	8
Length of large stator tooth h_{12} /mm	17	13–20	13.7
Radian of rotor tooth θ_1 /degrees	4	2–10	6
Radian of PM on small stator θ_2 /degrees	10	5–15	10
Radian of PM on large stator θ_3 /degrees	10	5–15	10.9
Radian of iron of stator yoke θ_4 /degrees	10	5–15	7.1

**Figure 5.** Flow chart of optimization.

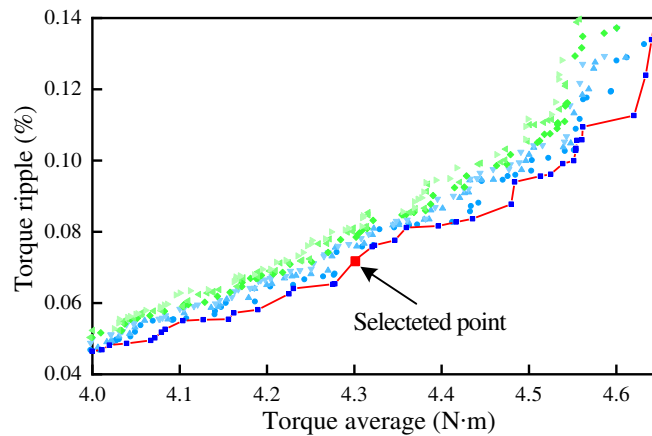


Figure 6. Pareto front of MOGA.

5. COMPARISON OF ELECTROMAGNETIC PERFORMANCE

5.1. Flux Density

The radial flux density in the air gap is shown in Figure 7(a). The amplitude of flux density of the proposed FRM is smaller than that of the conventional FRM. The reason is that the proposed model adopts the consequent pole structure; the consumption of PM is less than half of that of the conventional FRM; and the magnetomotive force provided by the PMs decreases. However, since the proposed FRM weakens the inter-pole flux leakage and its effective length of air gap is smaller, its amplitude of no-load flux linkage is higher than that of the conventional FRMs as shown in Figure 8. The amplitude of flux linkage of the conventional FRM is 0.103 Wb, and the amplitude of flux linkage of the proposed machine is 0.178 Wb, with an increase of 728%. The harmonic spectra of radial flux density in the air gap are shown in Figure 7(b). The main harmonics of the conventional FRM are 5th, 12th, 24th, 29th, and 48th, and the main harmonics of the proposed FRM are 5th, 6th, 12th, 18th, 24th, 29th, and 60th. The proposed machine has richer harmonics than the conventional FRM.

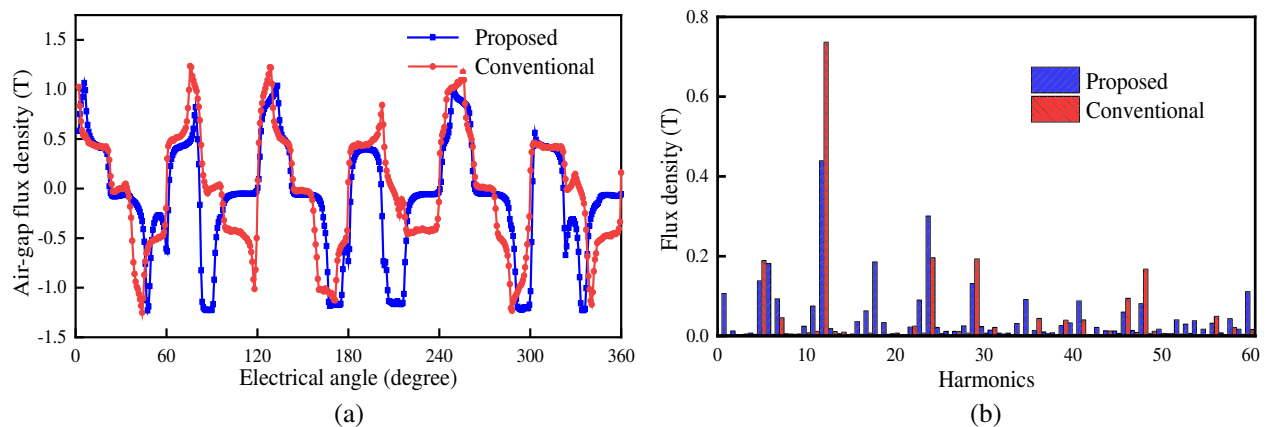


Figure 7. Radial flux density in the air gap. (a) Flux density distribution; (b) Harmonic spectra.

5.2. Back EMF

The back EMFs of the conventional FRM and the proposed FRM in one electric cycle are shown in Figure 9. Since the proposed machine can effectively reduce magnetic flux leakage, it has higher

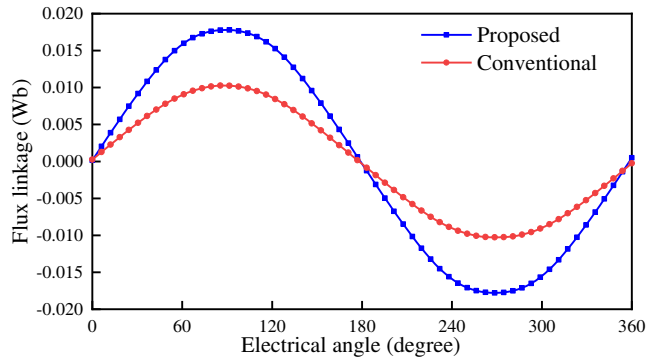


Figure 8. Flux linkage under no load condition.

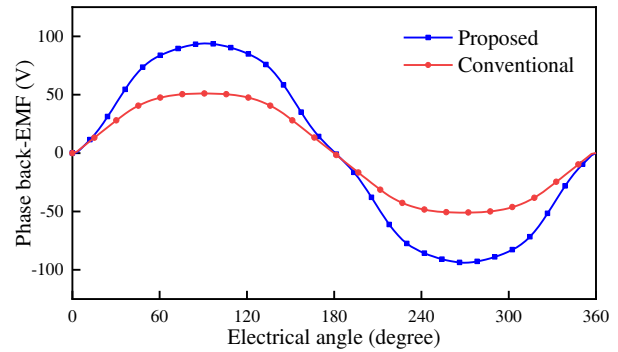


Figure 9. Back EMF under no load condition.

amplitude of each phase flux linkage and thus a higher amplitude of back EMF than the conventional FRM. The amplitude of back EMF of the conventional FRM is 50.98 V, and the amplitude of back EMF of the proposed machine is 93.88 V, with an increase of 84.15%. At the same time, the total harmonic distortion rate of back-EMF of the proposed machines is 4.44%, which is less than 13.53% of the conventional FRM. Therefore, the sinusoidal degree of the back EMF waveform of the proposed machine is higher than that of the conventional machine.

5.3. Torque

The electromagnetic torque can be obtained by using Maxwell stress tensor [20]. The electromagnetic torques of the conventional FRM and the proposed machines in one electric cycle are shown in Figure 10. The average torque of the proposed FRM is 4.33 N·m, which is 67.18% higher than 2.59 N·m of the conventional FRM. The torque density of the proposed FRMs is higher, and it can have greater output in a limited volume. The proposed machine adopts a consequent pole structure, so the consumption of PM is reduced by 51.6%. This indicates that per unit volume of PMs produces greater electromagnetic torque.

Since the effective air gap of the proposed FRM is smaller than that of the conventional FRM, the cogging effect is more obvious. The main flux of the proposed FRMs is larger, and the cogging torque is higher than that of the conventional FRM, which makes the proposed machine have greater torque ripple. The torque ripple of the conventional FRM is 3.61%, and the torque ripple of the proposed machine is 4.89%.

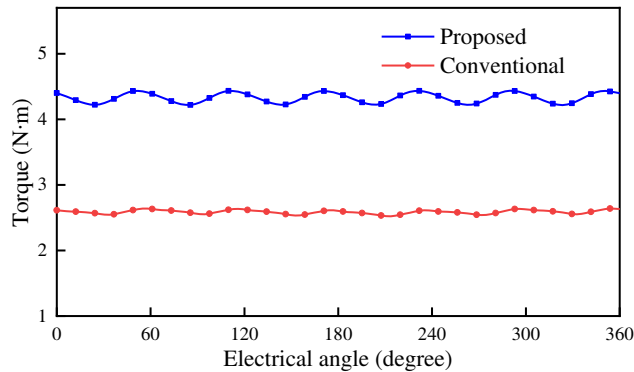


Figure 10. Electromagnetic torque.

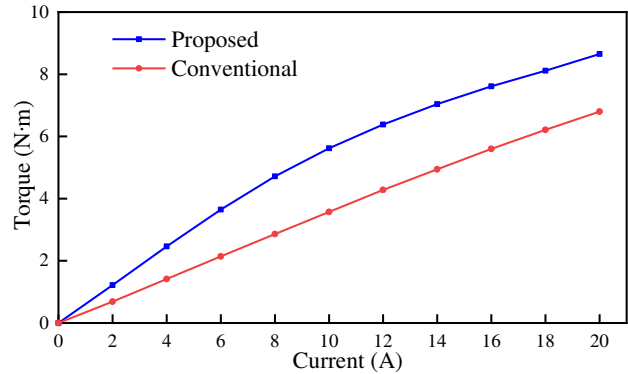


Figure 11. Torque versus current curves.

5.4. Overload Capability

To compare the overload capability of the two machines, the electromagnetic torque versus current curves is shown in Figure 11. As can be observed, the proposed machine is easier to reach saturation, and its overload capability is weaker than the conventional machine. This is mainly because the equivalent air gap of the proposed machine is smaller, resulting in a more intense armature reaction. However, the proposed machine can still provide higher torque at different currents and is suitable for applications where higher torque requirements are required.

6. CONCLUSION

In this paper, a novel consequent pole FRM with asymmetric stator teeth is presented. The principle of reducing magnetic flux leakage by the proposed machine is analyzed. Then, the genetic algorithm is used to globally optimize the design parameters to improve the performances of torque. The electromagnetic performances of the proposed FRM and the conventional FRM are analyzed and compared. The contributions of this study are summarized as follows.

- (1) Compared with the conventional machine, with less magnetic flux leakage and a smaller equivalent air gap, the amplitude of back EMF of the proposed machine is increased by 84.15%, and the total harmonic distortion is smaller. The proposed machine has a waveform with higher sinusoidal degree.
- (2) Compared with the conventional machine, the consumption of PM of the proposed machine is reduced by 51.6%, and the torque is increased by 67.18%. The torque ripple of the proposed machine is 4.89%, larger than 3.61% of the conventional FRM.
- (3) The proposed machine can produce greater average torque under different load conditions and is a strong candidate for occasions requiring high torque density.

REFERENCES

1. Cheng, M., W. Hua, J. Zhang, and W. Zhao, "Overview of stator-permanent magnet brushless machines," *IEEE Trans. Ind. Electron.*, Vol. 58, No. 11, 5087–5101, Nov. 2011.
2. Gao, Y., D. Li, R. Qu, X. Fan, J. Li, and H. Ding, "A novel hybrid excitation flux reversal machine for electric vehicle propulsion," *IEEE Trans. Veh. Technol.*, Vol. 67, No. 1, 171–182, Jan. 2018.
3. Gao, Y., R. Qu, D. Li, and J. Li, "Torque performance analysis of three-phase flux reversal machines," *IEEE Trans. Ind. Appl.*, Vol. 53, No. 3, 2110–2119, 2017.
4. Hua, W., X. Zhu, and Z. Wu, "Influence of coil pitch and stator-slot/rotor-pole combination on back EMF harmonics in flux-reversal permanent magnet machines," *IEEE Trans. Energy Conversion.*, Vol. 33, No. 3, 1330–1341, 2018.
5. Zhu, X., W. Hua, W. Wang, and W. Huang, "Analysis of back-EMF in flux-reversal permanent magnet machines by air gap field modulation theory," *IEEE Trans. Ind. Electron.*, Vol. 66, No. 5, 3344–3355, 2019.
6. Li, H. and Z. Zhu, "Optimal number of magnet pieces of flux reversal permanent magnet machines," *IEEE Trans. Energy Convers.*, Vol. 34, No. 2, 889–898, 2019.
7. Li, D., Y. Gao, R. Qu, J. Li, Y. Huo, and H. Ding, "Design and analysis of a flux reversal machine with evenly distributed permanent magnets," *IEEE Trans. Ind. Appl.*, Vol. 54, No. 1, 172–183, 2018.
8. Xie, K., D. Li, R. Qu, Z. Yu, Y. Gao, and Y. Pan, "Analysis of a flux reversal machine with quasi-halbach magnets in stator slot opening," *IEEE Trans. Ind. Appl.*, Vol. 55, No. 2, 1250–1260, 2019.
9. Qu, H., Z. Zhu, and H. Li, "Analysis of novel consequent pole flux reversal permanent magnet machines," *IEEE Trans. Ind. Appl.*, Vol. 57, No. 1, 382–396, Jan. 2021.
10. Yang, H., H. Lin, Z. Zhu, S. Lyu, and Y. Liu, "Design and analysis of novel asymmetric-stator-pole flux reversal pm machine," *IEEE Trans. Ind. Electron.*, Vol. 67, No. 1, 101–114, 2020.

11. Li, H., Z. Zhu, and H. Hua, "Comparative analysis of flux reversal permanent magnet machines with toroidal and concentrated windings," *IEEE Trans. Ind. Electron.*, Vol. 67, No. 7, 5278–5290, 2020.
12. Qu, H. and Z. Zhu, "Analysis of spoke array permanent magnet flux reversal machines," *IEEE Trans. Energy Convers.*, Vol. 35, No. 3, 1688–1696, 2020.
13. Wu, L., Y. Zheng, Y. Fang, and X. Huang, "Novel fault-tolerant doubly fed flux reversal machine with armature windings wound on both stator and rotor teeth," *IEEE Trans. Ind. Electron.*, Vol. 68, No. 6, 4780–4789, 2021.
14. Zheng, Y., L. Wu, J. Zhu, Y. Fang, and L. Qiu, "Analysis of dual-armature flux reversal permanent magnet machines with Halbach array magnets," *IEEE Trans. Energy Convers.*, Vol. 36, No. 4, 3044–3052, 2021.
15. Gao, Y., D. Li, R. Qu, and J. Li, "Design procedure of flux reversal permanent magnet machines," *IEEE Trans. Ind. Appl.*, Vol. 53, No. 5, 4232–4241, Sep.–Oct. 2017.
16. Gao, Y., R. Qu, D. Li, J. Li, and L. Wu, "Design of three-phase flux-reversal machines with fractional-slot windings," *IEEE Trans. Ind. Appl.*, Vol. 52, No. 4, 2856–2864, 2016.
17. Liu, G., Z. Ma, H. Zhu, J. Sun, and J. Huan, "Multi-objective optimization and analysis of six-pole outer rotor hybrid magnetic bearing," *Progress In Electromagnetics Research C*, Vol. 119, 97–114, 2022.
18. Jing, L., W. Tang, W. Liu, Y. Rao, C. Tan, and R. Qu, "A double-stator single-rotor magnetic field modulated motor with HTS bulks," *IEEE Trans. Appl. Supercond.*, Vol. 32, No. 6, 1–5, 2022.
19. Tang, W., L. Jing, and L. Zheng, "A diesel-electric hybrid field modulation motor with bread-loaf eccentric magnetic pole for ship propulsion," *Progress In Electromagnetics Research C*, Vol. 125, 147–159, 2022.
20. Zhou, X., X. Zhu, W. Wu, Z. Xiang, Y. Liu, and L. Quan, "Multi-objective optimization design of variable-saliency-ratio PM motor considering driving cycles," *IEEE Trans. Ind. Electron.*, Vol. 68, No. 8, 6516–6526, Aug. 2021.